IPPI

Polyolefins Journal, Vol. 13, No. 1 (2026)
DOI: 10.22063/poj.2025.35787.1376

ORIGINAL PAPER

Ethylene polymerization using MAO-free catalyst system consisting of alkylaluminum and zirconocene supported on acid-treated montmorillonite

Hideki Kurokawa*, Shou Kikuchi, Hiroshi Miura

Graduate School of Science & Engineering, Saitama University
255, Shimo-Okubo, Sakura-ku, Saitama-shi, Saitama, 338-8570 Japan

Received: 8 October 2025, Revised: 17 December 2025, Accepted: 30 December 2025

ABSTRACT

MAO-free supported catalysts for ethylene polymerization were prepared by sequentially treating montmorillonites (MMTs) with R_3Al and then with zirconocene. MMTs possessing different physicochemical properties—such as surface area, acidity, and crystallinity—were employed for catalyst preparation. Three zirconocenes, Cp_2ZrCl_2, $(1,3\text{-}Me_2Cp)_2ZrCl_2$, and $Me_2Si(Cp)_2ZrCl_2$, were used. Acid treatment of raw MMT (Na^+-montmorillonite) increased the surface area while decreasing both the Al content and crystallinity. The maximum surface area (316 $m^2\ g^{-1}$) was obtained when the residual Al content was 18%. The effects of triethylaluminum (TEA) and triisobutylaluminum (TIBA) on catalyst performance were investigated. Although treatment of surface OH groups was necessary to obtain the zirconocene-supported catalysts with high activity, no significant difference in catalytic activity was observed between TEA- and TIBA-treated MMTs. In contrast, the type of R_3Al used as a scavenger during polymerization strongly influenced catalytic activity: catalysts employing TEA exhibited much lower activity than those using TIBA. Since TEA is a stronger Lewis acid than TIBA, it likely coordinates more strongly to the active sites, thereby acting as an inhibitor. Therefore, TIBA was employed in all subsequent experiments. The catalytic activity, based on catalyst weight, increased with both surface area and the amount of supported zirconocene, reaching a maximum when the residual Al content was 54%. A linear correlation between the activity (per catalyst weight) and the amount of supported zirconocene was observed for two zirconocenes, Cp_2ZrCl_2 and $(1,3\text{-}Me_2Cp)_2ZrCl_2$, indicating that the supported zirconocenes functioned uniformly as active species for ethylene polymerization. However, 5-7 μmol g^{-1}-cat of zirconocene formed inactive species in both catalysts. Unusual behavior was observed for the supported $Me_2Si(Cp)_2ZrCl_2$ catalysts: at higher residual Al content, the correlation was similar to that of the other two catalysts, whereas at lower residual Al content, most of the supported zirconocene formed inactive species, and only a small fraction acted as active sites. We speculate that $Me_2Si(Cp)_2ZrCl_2$ is difficult to activate, and that only the species formed by reaction of strong acid sites with R_3Al can specifically activate this complex. **Polyolefins J (2026) 13: 1-11**

Keywords: Metallocene catalyst; ammonia adsorption; layered aluminosilicate; methylaluminoxane; olefin polymerization.

INTRODUCTION

Polyethylene (PE) is the most extensively produced resin worldwide and is used in a wide range of applications, including films, sheets, bottles, and pipes [1]. In the early 20th century, PE was synthesized via radical polymerization under extremely high ethylene pressures (>1000 bar). In 1960, Ziegler and co-workers reported titanium chloride-based catalysts, hereafter referred to as "Ziegler catalysts," which enabled ethylene polymerization under significantly milder conditions [2].

The discovery by Sinn and Kaminsky in 1980 of an α-olefin polymerization catalyst comprising a Group IV metallocene complex and methylaluminoxane (MAO) as a cocatalyst [3] initiated extensive investigations, as the microstructure of polyolefins can be precisely tailored by selecting an appropriate metallocene complex [4-7]. Within this system, MAO functions as an activator by generating cationic complexes and stabilizing the cationic metal center through weak, noncoordinating interactions. MAO is a mixture of oligomers containing 4-12 aluminum atoms, synthesized via partial hydrolysis of trimethylaluminum. Consequently, the

*Corresponding Author - E-mail: kuro@apc.saitama-u.ac.jp

CC BY NC SA

correlation between the molecular structure and the function of MAO has been intensively examined. A significant advance was the identification of Lewis acidic compounds, such as tris(pentafluorophenyl) borane [8-10], as effective cocatalysts for metallocene activation, yielding highly active catalysts for ethylene and propylene polymerization.

For implementation in industrial slurry- and gas-phase polymerization processes, metallocene complexes and/or cocatalysts must be immobilized on support materials. Numerous supported metallocene catalysts have been developed [11,12]. One notable approach involves the use of alkylaluminum compounds, such as triethylaluminum (TEA) and triisobutylaluminum (TIBA), in place of MAO for catalyst activation. Kaminaka and Soga reported MAO-free systems consisting of Al_2O_3- or $MgCl_2$-supported $Et(H_4Ind)_2ZrCl_2$ in combination with AlR_3 ($R = CH_3$, C_2H_5) for propylene polymerization [13,14].

Supported zirconocene catalysts as MAO-free systems have also been extensively investigated for ethylene polymerization. Examples include zirconocene supported on halo organoaluminum- and dialkylmagnesium-modified SiO_2 [15], R_3Al-treated aerogel [16], R_3Al-treated $MgCl_2$ [17,20], trimethylaluminum (TMA)- and fluorinated sultone-modified SBA-15 [18], R_3Al-treated $AlPO_4$ [19], Mg-, Na-, and Li-modified SiO_2 [21], fluorinated TMA-treated SiO_2 [22,23], ionic liquid-modified SiO_2 [24], and fluorinated Al_2O_3 [25].

Suga *et al*. proposed a cocatalyst/support system based on montmorillonite (MMT), a layered aluminosilicate (clay mineral), which functions as both a cocatalyst and a support for metallocene complexes [26,27]. Metallocene complexes supported on clay minerals exhibited high activity in ethylene and propylene polymerization when activated with conventional alkylaluminum compounds (e.g., TEA, TIBA), without the use of MAO. As clay minerals are solid materials, the supported catalysts can be readily prepared and applied in gas- and slurry-phase processes, which dominate commercial PE production. They termed MMT promoted by physicochemical modification a "support activator."

Weiss *et al*. concluded that active sites for zirconocene activation were generated by the reaction of R_3Al with Si-OH groups on silica arms (dendrimer-like silica) formed by the acid treatment of MMT [28]. The acidity of MMT [29] and the textural characteristics of aluminum species formed on its surface [30] were found to influence catalytic activity. Tayano *et al*. reported high activity in propylene polymerization using zirconocene supported on acid-treated MMT, concluding that strong acid sites ($pKa < -8.2$) on the MMT surface were required for the formation of highly active sites [31].

We previously reported the preparation of a fluorotetrasilicic mica-supported metallocene catalyst and its application in ethylene slurry polymerization. Fluorotetrasilicic mica is a layered aluminosilicate exhibiting structural and physicochemical features analogous to those of MMT. In this system, the swelling behavior of cation-exchanged mica directly influenced catalytic activity, as exfoliation of the mica layers was necessary to achieve high activity [32]. In this paper, we investigated the role of MMT as a "support activator" in the catalyst performance using three types of zirconocene complexes (Figure 1) and acid-treated MMTs with different Al contents and surface areas. In particular, the effects of the Al content of MMT, the amount of supported zirconocene, and the amount of acid sites on the catalytic activity were systematically investigated.

EXPERIMENTAL

All solvents and reagents were purchased from Kanto Chemical Corporation. MMT (JCSS-3102) was obtained from the Clay Science Society of

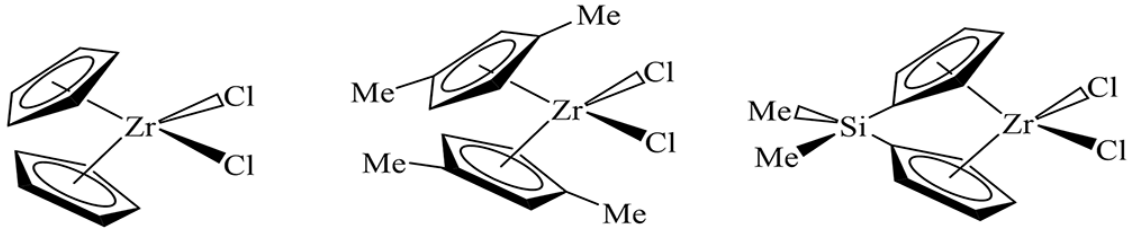

(a) Cp_2ZrCl_2 (b) $(1,3\text{-}Me_2Cp)_2ZrCl_2$ (c) $Me_2Si(Cp)_2ZrCl_2$

Figure 1. zirconocene complexes used in this study.

Japan. Toluene and n-hexane were used for catalyst preparation and ethylene polymerization after dehydration with MS-13X, calcined at 400°C for 5 h under reduced pressure.

Acid-treatment of MMT

MMT was treated with an aqueous H_2SO_4 solution (3.0 mol L^{-1}; 25 mL of solution per gram of MMT) at 30-90°C for 24 h. The product was washed with deionized water and ethanol, calcined at 300°C for 4 h, and subsequently dried under reduced pressure at 300°C for an additional 4 h. Our preliminary results indicated that the catalytic activity decreased when the drying temperature of the acid-treated MMT increased from 200 to 400ºC. Although the catalyst prepared using the MMT dried at 200ºC exhibited the highest activity, its activity varied among repeated runs. These findings suggested that residual weekly bonded water might influence the catalytic activity. Therefore, a drying temperature of 300ºC was adopted to ensure high reproducibility in polymerization performance. The resulting acid-treated MMT (denoted as H^+-mont-X) was stored under a nitrogen atmosphere and used for catalyst preparation, where X indicates the percentage of residual Al relative to that in Na^+-mont. The chemical composition and crystallinity of H^+-mont-X were determined by X-ray fluorescence (XRF, Spectris Co., Ltd., PW 2400) and X-ray diffraction (XRD, Rigaku K.K., Ultima III), respectively. The surface acidity of H^+-mont-X was quantified by NH_3 chemisorption using a static adsorption apparatus. Surface morphology was examined by scanning electron microscopy (SEM, Hitachi High-Technologies Corporation, S-4100). The specific surface area of the prepared MMTs was determined by a BET method using SA-6200 (HORIBA, Ltd.).

Preparation of supported catalysts

All procedures described below were performed under a nitrogen atmosphere. In a 50-mL Schlenk flask, 20 mg of H^+-mont-X was weighed in a glove box. Toluene (20 mL) and alkylaluminum (TEA or TIBA, 95 μmol-Al g-mont^{-1}) were subsequently added. The slurry was stirred for 1 min and then allowed to stand for 90 min at ambient temperature. Most of the solution was removed with a syringe, and the solid was washed with fresh toluene under stirring. This washing process was repeated four times to remove unbound alkylaluminum.

A toluene solution of zirconocene was then added to the slurry (100 μmol g-mont^{-1}), and the mixture was allowed to react with TIBA- or TEA-treated H^+-mont-X for 60 min at ambient temperature. The solution containing unbound zirconocene was removed with a syringe, and the solid was repeatedly washed with fresh toluene to eliminate weakly adsorbed zirconocene species. The resulting zirconocene-supported H^+-mont-X was used for polymerization in the form of a toluene slurry. The zirconocene loading was determined by XRF analysis, calibrated using standard samples prepared by impregnation of H^+-mont-X with a toluene solution of zirconocene complexes.

Polymerization of ethylene

n-Hexane (10 or 50 mL), the catalyst toluene slurry (2.0-8.0 mg based on catalyst), and a 0.25 M TIBA or TEA toluene solution were successively introduced into a stainless-steel autoclave equipped with a magnetic stirrer. The autoclave had an internal volume of 30 mL when using the Cp_2ZrCl_2- and $Me_2Si(Cp)_2ZrCl_2$-supported catalysts, and 120 mL when using the $(1,3\text{-}Me_2Cp)_2ZrCl_2$-supported catalyst. The catalyst amount and the Al/Zr ratio during polymerization were adjusted to their optimal values based on the results of preliminary experiments. These values are shown in each figure. The larger reactor (120 mL) was used for polymerization with the supported $(1,3\text{-}Me_2Cp)_2ZrCl_2$ catalysts because these catalysts exhibited exceedingly high activity. This was necessary to avoid monomer transfer limitations and to ensure proper control of the reaction temperature.

Based on the results of preliminary experiments, the polymerization temperature and ethylene pressure were also selected to adjust the average-number molecular weight (M_n) of the resulting polyethylene to approximately 10^5. The autoclave was purged with ethylene and then immersed in a water bath maintained at 60°C. Ethylene pressure was adjusted to the desired value and maintained by continuous ethylene feeding during polymerization. The applied ethylene pressures were 0.7 MPa for the Cp_2ZrCl_2- and $(1,3\text{-}Me_2Cp)_2ZrCl_2$-supported catalysts, and 0.4 MPa for the $Me_2Si(Cp)_2ZrCl_2$-supported catalyst.

After the reaction, the residual ethylene was vented, and the resulting polyethylene was collected by filtration as a powder. The obtained PE was dried and weighed to determine the catalysis-based activity. The molecular weight and its distribution were analyzed by gel permeation chromatography (GPC, ALC/GPC 150C, Waters Corporation).

RESULTS AND DISCUSSION

Characterization of H$^+$-mont-X

Acid treatment induces dealumination from the octahedral sheets of MMT, resulting in an increase in surface area and a decrease in crystallinity. Table 1 summarizes the physicochemical properties of H$^+$-mont samples prepared under various acid-treatment conditions of Na$^+$-mont. When the treatment temperature was increased from 30 to 90°C, the surface area of the resulting H$^+$-mont increased from 53 to 263 m^2 g^{-1}, accompanied by a concomitant decrease in Al content. The maximum surface area (316 m^2 g^{-1}) was obtained by treating Na$^+$-mont twice at 90°C. However, under more severe conditions (100°C, twice), the surface area of H$^+$-mont decreased to 276 m^2 g^{-1}. The decreased surface area of MMT-8 was attributable to the formation of amorphous silica, which typically exhibits a relatively small surface area (~200 m^2 g^{-1}).

The XRD profiles of Na$^+$-mont and the acid-treated MMTs are shown in Figure 2. Because the purchased Na$^+$-mont (raw material) is a natural product, some impurities were present. In the XRD profiles of the raw material, quartz was identified as a typical impurity, as evidenced by the peak observed at 2θ = 26°. The intensity of the peaks attributed to MMT markedly decreased with increasing acid-treatment temperature due to dealumination. After two acid treatments at 90°C, the peak intensity of the resulting H$^+$-mont-25 almost disappeared, while the halo peak corresponding to amorphous SiO_2 became more pronounced. Under the harshest treatment conditions, the peaks corresponding to MMT disappeared completely. Dealumination from the octahedral sheets destroyed the crystal structure of MMT, thereby increasing its surface area.

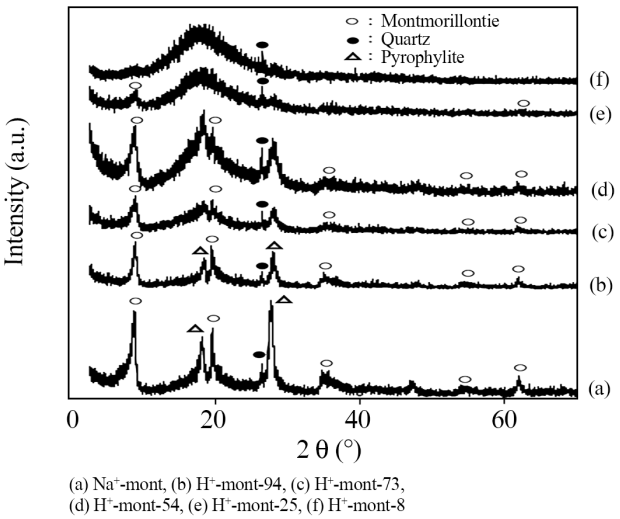

(a) Na$^+$-mont, (b) H$^+$-mont-94, (c) H$^+$-mont-73, (d) H$^+$-mont-54, (e) H$^+$-mont-25, (f) H$^+$-mont-8

Figure 2. XRD profiles of Na$^+$- and H$^+$-mont-X.

The surface morphology of H$^+$-mont-X (X = 94, 77, 54, 31, and 8) was examined by SEM, and the corresponding micrographs are presented in Figure 3. The SEM image of H$^+$-mont-94 (photo (a)) clearly showed the characteristic sheet-like morphology associated with the lamellar structure of MMT. In contrast, although the sheet-like morphology remained discernible in photos (b) and (c), particles smaller than 50 nm were distinctly observed on the sheet surfaces. For H$^+$-mont-31 (photo (d)), the surface was predominantly covered with numerous small particles (right side of the photo), while only limited remnants of the original sheet-like structure were observed (left side of the photo). A more pronounced change was observed in H$^+$-mont-8 (photo (e)), which had the lowest Al content and was obtained under the most severe acid-treatment conditions. In this case, the original sheet-like morphology had almost completely disappeared, giving rise to a surface dominated by aggregated particles. Based on combined XRD, XRF, and SEM analyses,

Table 1. Physicochemical properties of acid-treated montmorillonite.

Support	Acid-treatment conditions *1		Residual Al content (%) *2	Surface area (m^2 g^{-1}) *3	Pore diameter (nm)
	Temperature (ºC)	Number of treatment			
Na$^+$-mont	-	-	100	14	22.6
H$^+$-mont-94	30	1	94.4	53	8.8
H$^+$-mont-88	60	1	88.4	124	9.7
H$^+$-mont-77	80	1	76.5	205	11.1
H$^+$-mont-54	90	1	54.3	263	12.5
H$^+$-mont-31	80	2	30.8	292	-
H$^+$-mont-25	90	2	25.1	309	19.0
H$^+$-mont-18	90	2	18.2	316	-
H$^+$-mont-8	100	2	7.9	276	25.9

*1 3 M H_2SO_4 aqueous solution was used. *2 Determined by XRF. *3 Determined by BET method.

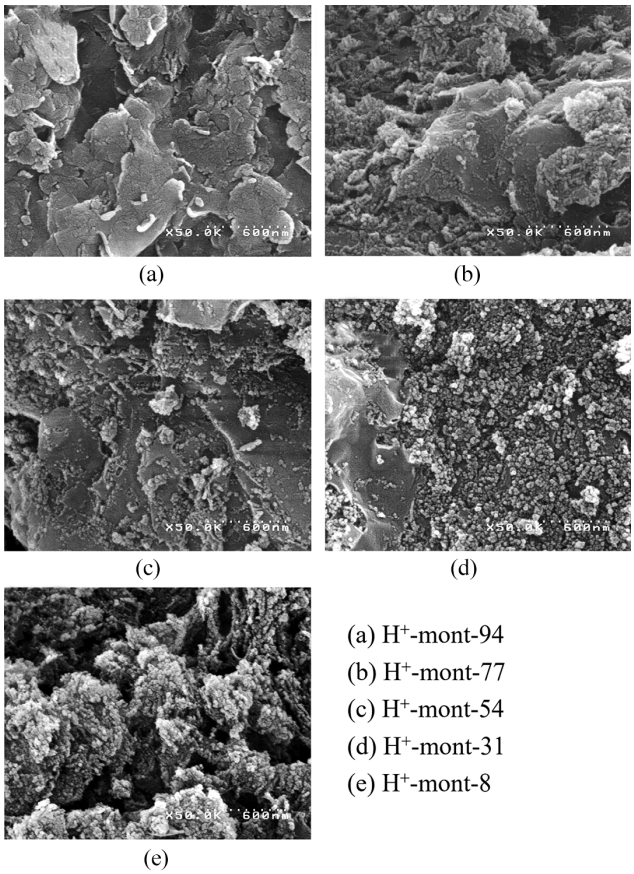

Figure 3. SEM images of Na^+- and H^+-mont-X.

these particles were attributed to arm-like amorphous silica chain generated via extensive dealumination of the MMT framework. This interpretation is consistent with the findings of Weiss *et al*. [28], who reported that dealumination preferentially occurred at the edges of MMT lamellae, leading to the formation of amorphous SiO_2 dendrimers.

The acidity of the prepared H^+-mont samples was evaluated using a conventional static NH_3 adsorption method, and the results are presented in Figure 4. Adsorption measurements were carried out at two temperatures (room temperature and 100°C). Because NH_3 is a strong base, the amount adsorbed at room temperature likely includes contributions from non-acidic silanol groups. In contrast, NH_3 desorbing at higher temperature is more strongly bound to acid sites, and thus the amount of NH_3 adsorbed at 100°C can be regarded as a measure of stronger acid sites.

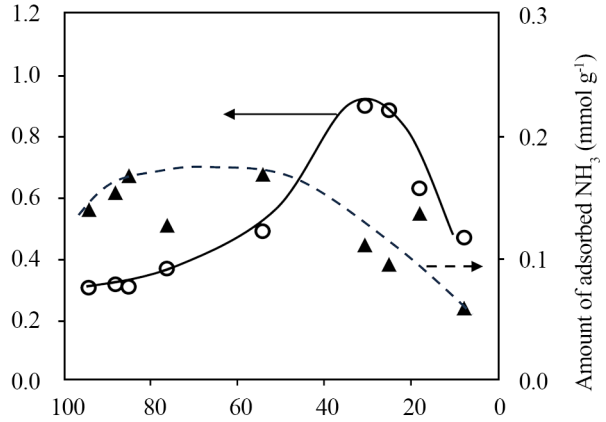

Figure 4. Relationship between residual Al content and amount of NH_3 adsorbed on H^+-mont-X.

The amount of acid sites determined from adsorption at room temperature increased with decreasing Al content, reaching a maximum value of 0.90 mmol g-mont^{-1} at an Al content of 30.8 wt.%. These acid sites are primarily silanol groups adjacent to Al atoms, and their amount depends on both the Al content in the aluminosilicate framework and the surface area of H^+-mont. At higher Al contents, the effect of the increased surface area outweighed that of the decreasing Al content. Consequently, the amount of weaker acid sites per gram of H^+-mont increased with decreasing Al content. Around the maximum surface area, however, the acidity decreased owing to the relatively small variation in surface area. The amount of NH_3 adsorption at 100°C showed little change up to an Al content of 50% and gradually decreased below this threshold, a trend attributed to the loss of crystallinity in MMT.

Effects of R_3Al treatment of H^+-mont-54 on catalytic activity

The effects of R_3Al treatment of H^+-mont-X on catalyst performance were investigated, and the results are summarized in Table 2. When the zirconocene complex was directly supported on untreated H^+-mont-54, the catalytic activity for ethylene polymerization was observed (entries 1 and 2), irrespective of the type of R_3Al. Severn *et al*. [9] proposed the formation of two types of inactive surface species: one with a single Si-O-Zr bond and another with two Si-O-Zr bonds, generated by the reaction of metallocene complexes with surface silanol groups. They also reported that the former species can be readily activated with MAO, whereas the latter species is essentially inactive for alkene polymerization. The low activity of the catalysts supported on untreated H^+-mont-54 is therefore attributed to the formation of those inactive species.

Employing TEA as a scavenger exhibited much lower activity than those using TIBA. Since TEA is a stronger Lewis acid than TIBA, it likely coordinated more strongly to the active sites, thereby acting as an inhibitor. The inhibitory effect of TEA was also

Table 2. Effect of R_3Al treatment of H^+-mont-54 on catalytic activity.

Entry	R_3Al Treatment *1	Scavenger *2	Supported Cp_2ZrCl_2 (mmol g-cat^{-1})	Activity (g-PE g-cat^{-1} hr^{-1})
1	none	TIBA	20.4	95
2	none	TEA	17.5	21
3	TIBA	TIBA	24.3	351
4	TEA	TIBA	33.6	326
5	TIBA	TEA	21.9	80
6	TEA	TEA	33.5	65

*1 R_3Al used for treatment of H^+-mont-54 before supporting Cp_2ZrCl_2.
*2 R_3Al used during polymerization.

evident when R_3Al was used for the pretreatment of H^+-mont-54: the amount of supported complex was significantly higher for the TEA-treated catalyst than for the TIBA-treated one. Interestingly, the kind of R_3Al employed as a scavenger had more pronounced influence on catalytic activity, most likely because an excess amount of the scavenger was present during polymerization.

The deactivation mechanism of MAO-free zirconocene catalysts employing alkylaluminum activators was investigated in detail by Tyumkina *et al*. using computational analysis [33-35]. They concluded that, when TEA is used as an activator in MAO-free systems, unstable diethyl zirconocene (Cp_2ZrEt_2) predominantly undergoes ethane elimination to form zirconia cyclopropane species, which are inactive toward alkene insertion. In contrast, the reaction of zirconocene dichloride with diisobutylaluminum hydride leads readily to the formation of an intermediate composed of chain-like trialuminum species coordinated with zirconocene, which remains active for ethylene insertion. In our study, the low activity observed when using TEA as an activator may likewise be attributed to the formation of such inert species.

Based on our observations and the results reported by Tyumkina *et al*., TIBA was employed as both the pretreatment agent and scavenger in all subsequent experiments.

Polymerization using Cp_2ZrCl_2, $(1,3\text{-}Me_2Cp)_2ZrCl_2$, and $Me_2Si(Cp)_2ZrCl_2$ supported on H^+-mont-X

The supported catalysts consisting of Cp_2ZrCl_2 and H^+-mont-X were evaluated, and the results are presented in Figure 5. Figure 5(a) shows the catalytic activity of these catalysts along with the amount of supported Cp_2ZrCl_2 measured by XRF. Both the catalytic activity and the amount of the supported zirconocenes exhibited volcano-type trends with respect to the Al content (Figure 5(a)). A linear correlation between the amount of supported zirconocenes and the catalytic activity was observed (Figure 5(b)), indicating that the supported zirconocenes exhibited identical intrinsic activity for ethylene polymerization. Closer inspection of Figure 5 (b) reveals that the linear trendline did not

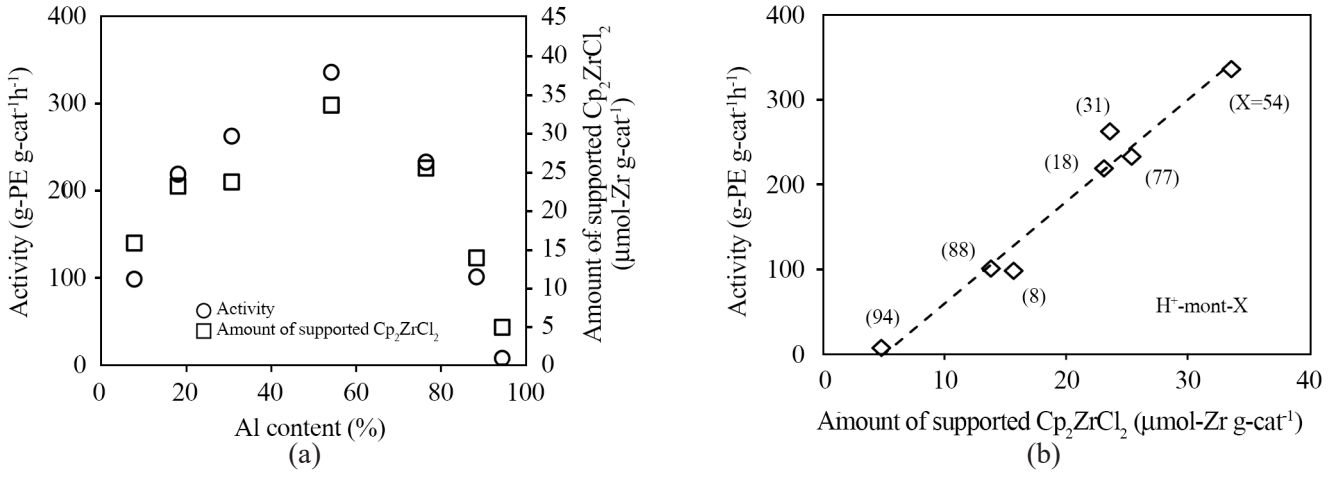

Figure 5. Ethylene polymerization using Cp_2ZrCl_2 supported on R_3Al-treated H^+-mont-X. Reaction conditions: ethylene pressure = 0.7 MPa; reaction temperature = 60ºC; catalyst = 2.0 mg (X = 18, 31, 54, 77, and 88) and 3.0 mg (X = 8 and 94); TIBA = 0.18 mmol (X = 18, 31, 54, 77, and 88) and 0.27 mmol (X = 8 and 94). The values in parentheses represent the residual aluminum content X.

pass through the origin, suggesting that approximately 5 μmol of the supported zirconocenes were inactive for polymerization, despite pretreatment of the H^+-mont-X surface with an alkyl aluminum. Since these inactive zirconocenes were not removed by washing with toluene, they appear to have a strong interaction with the surface of H^+-mont-X. Based on the slope obtained in Figure 5(b), the catalytic activity was estimated as 2.0×10^7 g-PE mol-Zr^{-1} h^{-1} at 0.7 MPa.

The molecular weight and molecular weight distribution of the synthesized polyethylene were determined by GPC. The values were typically in the range of M_n = (1.1-1.3) × 10^5 and M_w/M_n = 2.4-2.9. These values were characteristic of polyethylene synthesized using zirconocene catalysts, although slight variations were observed owing to the use of a small reactor with limited controllability.

Figure 6 presents the results of polymerization using $(1,3\text{-}Me_2Cp)_2ZrCl_2$ supported on H^+-mont-X. The catalytic activity and the amount of supported zirconocenes showed the same trends as those observed for Cp_2ZrCl_2 supported on H^+-mont-X. A linear correlation was again observed in Figure 6(b), though with slightly lower linearity compared to Figure 5(b). The trendline did not pass through the origin, consistent with the previous observation. Based on the slope, the catalytic activity was estimated as 2.5×10^7 g-PE mol-Zr^{-1} h^{-1} at 0.4 MPa. The intrinsic activity per the supported $(1,3\text{-}Me_2Cp)_2ZrCl_2$ was much higher than that of Cp_2ZrCl_2.

Figure 7 shows the results of polymerization using the $Me_2Si(Cp)_2ZrCl_2$ supported on H^+-mont-X, a

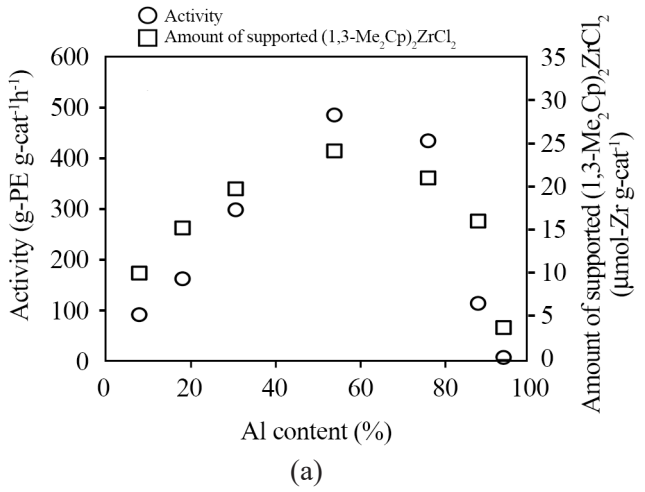

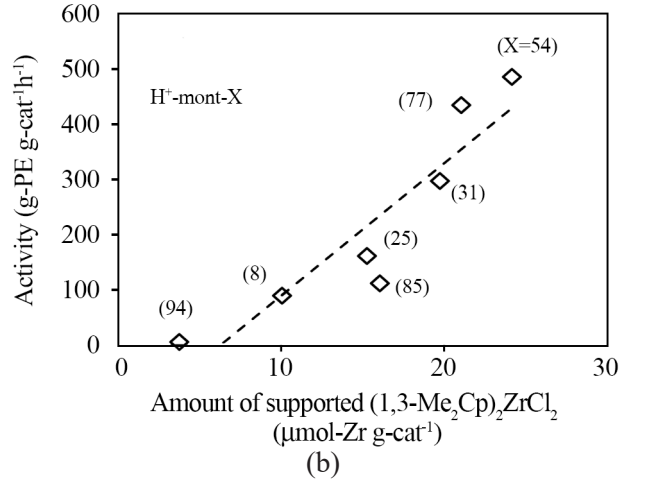

Figure 6. Ethylene polymerization using $(1,3\text{-}Me_2Cp)_2ZrCl_2$ supported on R_3Al-treated H^+-mont-X. Reaction conditions: ethylene pressure = 0.4 MPa; reaction temperature = 60°C; catalyst = 2.0 mg (X = 8, 25, 31, 54, 77, and 85) and 3.0 mg (X = 94); TIBA = 0.24 mmol (X = 8, 25, 31, 54, 77, and 85) and 0.36 mmol (X = 94). The values in parentheses represent the residual aluminum content X.

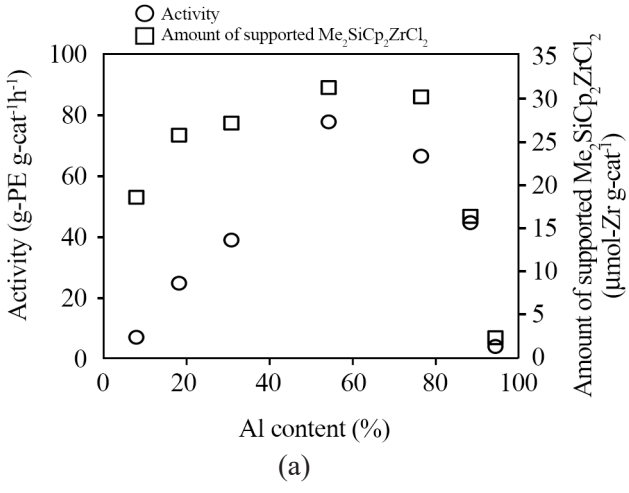

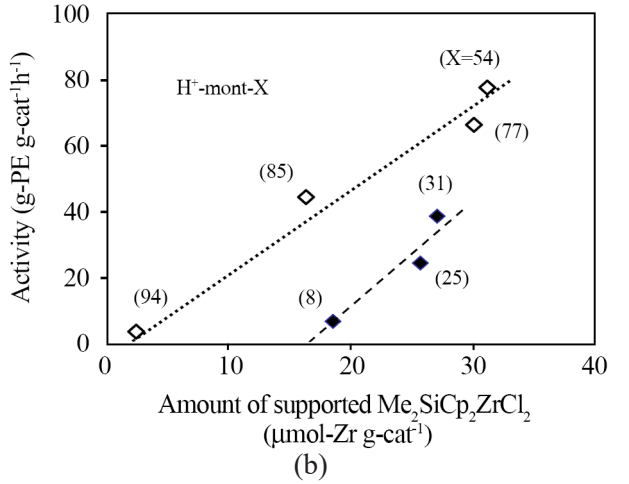

Figure 7. Ethylene polymerization using $Me_2Si(Cp)_2ZrCl_2$ supported on R_3Al-treated H^+-mont-X. Reaction conditions: ethylene pressure = 0.7 MPa; reaction temperature = 60°C; catalyst = 6.0 mg (X = 8, 25, 31, 54, 77, and 85) and 8.0 mg (X = 94); TIBA = 0.18 mmol (X = 8, 25, 31, 54, 77, and 85) and 0.24 mmol (X = 94). The values in parentheses represent the residual aluminum content X.

bridged-type zirconocene. The prepared catalysts exhibited significantly lower activity than the two non-bridged zirconocene catalysts. Notably, two distinct correlations (dashed and dotted lines) were observed in Figure 7(b), representing the relationship between the amount of supported zirconocenes and the catalytic activity. These correlations depended on the residual Al content in H^+-mont-X: the catalysts with higher Al content (X = 94-54) showed higher activity based on the catalyst amount than those with lower Al content (X = 31-8). The dashed-line trend in Figure 7(b) suggests that approximately 17 μmol-Zr g-cat^{-1} of zirconocene supported on low-Al-content H^+-mont-X formed inactive species.

The trend in ethylene consumption during polymerization is shown in Figure 8. Similar profiles were observed for the polymerizations conducted using the MMT-supported Cp_2ZrCl_2 and $(1,3\text{-}Me_2Cp)_2ZrCl_2$ catalysts. After the rapid initial drop in ethylene uptake attributable to ethylene absorption into the solvent, the consumption rate gradually increased as polymerization progressed, and then slowly decreased after approximately 40 min. In contrast, a long induction period and a low ethylene consumption rate were observed during the polymerization using the MMT-supported $Me_2Si(Cp)_2ZrCl_2$ catalyst; this catalyst system was difficult to be activated under the present polymerization conditions.

Activation mechanism of zirconocene with R_3Al-treated H^+-mont-X

Although no direct evidence has yet been obtained, an activation mechanism is proposed based on these results (Figure 9). $Me_2Si(Cp)_2ZrCl_2$ was more difficult to activate than Cp_2ZrCl_2 and $(1,3\text{-}Me_2Cp)_2ZrCl_2$. During the catalyst preparation, $Me_2Si(Cp)_2ZrCl_2$ was preferentially adsorbed at B sites, formed by the reaction of R_3Al with Si-OH groups on silica-like surface, leading to the formation of inactive species. After most B sites were occupied, only A sites – formed by the reaction of R_3Al with Si-OH groups adjacent to Al atoms, corresponding to strong acid sites- could effectively activate $Me_2Si(Cp)_2ZrCl_2$. This hypothesis is supported by the NH_3 adsorption data in Figure 4: the amount of strong acid sites, determined by NH_3 adsorption at 100°C, decreased with decreasing Al content. In contrast, both Cp_2ZrCl_2 and $(1,3\text{-}Me_2Cp)_2ZrCl_2$ could be readily activated at either A or B sites; thus, their catalytic activities per supported zirconocene were independent of the Al content in H^+-mont-X.

These findings are consistent with the results reported by Tayano *et al*. [31,36]. They demonstrated that the catalytic activity for propylene polymerization using more sterically hindered *ansa*-zirconocenes was well correlated with the surface area of acid-treated MMT, particularly with the surface area associated with pores having diameters below 6 nm, where strong acid sites are present. In their study, the residual aluminum content of the acid-treated MMT was in the range of 50-100% relative to that of the untreated material. In the present study, the catalytic activity for ethylene polymerization was also well correlated with the surface area within a similar range of residual aluminum content. In the higher surface-area region, the total surface area of MMT was nearly equal to the surface area contributed by small pores with diameters below 6 nm.

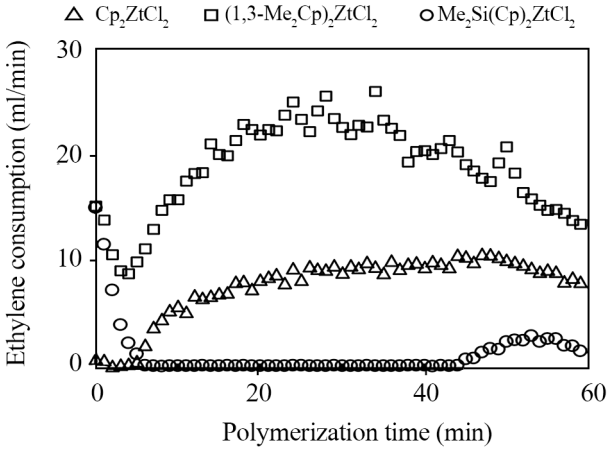

Figure 8. Ethylene consumption profiles during polymerization using three supported zirconocene catalysts. Reaction conditions: ethylene pressure = 0.7 MPa; reaction temperature = 60°C; MMT = H^+-mont-54; catalyst = 2.0 mg; TIBA = 0.24 mmol.

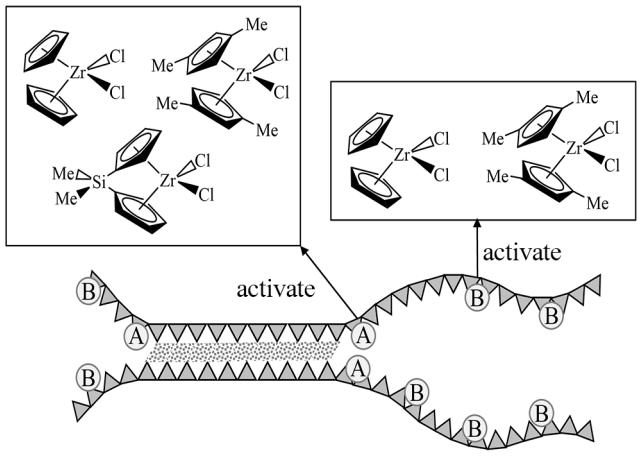

Figure 9. Proposed mechanism of zirconocene activation by R_3Al-treated H^+-mont-X.

In contrast, for acid-treated MMT with lower residual aluminum contents (below 31%) relative to the untreated material, no correlation between the catalytic activity and surface area was observed, even when MMT with a high surface area was used. The pore diameter of the acid-treated MMT increased with the severity of the acid-treatment conditions, leading to an overall increase in surface area. The catalytic activity showed no clear correlation with pore diameter, indicating that activation of the zirconocene species within the internal pores was not the dominant factor governing the catalytic performance.

These results indicated that strong acid sites decrease as a result of dealumination at lower residual aluminum contents. Therefore, only highly reactive sites formed through the interaction of strong acid sites with R_3Al are able to contribute effectively to the activation of zirconocenes possessing Si-bridged Cp rings (*ansa*-type zirconocenes).

CONCLUSION

Acid-treated montmorillonites (H^+-mont-X, where X denotes the residual Al content) with varying degree of dealumination were prepared and used as supports for zirconocene catalysts. The surface area of H^+-mont increased with decreasing Al content owing to the removal of aluminum from the octahedral sheets of MMT. Supported catalysts containing Cp_2ZrCl_2, $(1,3\text{-}Me_2Cp)_2ZrCl_2$, and $Me_2Si(Cp)_2ZrCl_2$ on H^+-mont-X were prepared, and their catalytic activities were evaluated in ethylene polymerization.

Pretreatment of H^+-mont with triethylaluminum (TEA) or triisobutylaluminum (TIBA) prior to zirconocene loading was effective for obtaining highly active catalysts, although no significant difference in catalytic activity was observed between TEA- and TIBA-treated MMTs. In contrast, the type of R_3Al used as a scavenger during polymerization strongly affected catalytic activity: catalysts employing TEA exhibited much lower activity than those using TIBA.

A linear correlation between activity (per catalyst weight) and the amount of supported zirconocene was observed for Cp_2ZrCl_2 and $(1,3\text{-}Me_2Cp)_2ZrCl_2$, indicating that the supported zirconocenes functioned uniformly as active species for ethylene polymerization. However, approximately 5-7 μmol g-cat^{-1} of zirconocene formed inactive species in both catalysts. Unusual behavior was observed for the supported $Me_2Si(Cp)_2ZrCl_2$ catalysts. At higher residual Al content, the correlation was similar to that of the other two catalysts, whereas at lower residual Al content, most of the supported zirconocene formed inactive species, and only a small fraction acted as active sites. The order of the maximum activity was $(1,3\text{-}Me_2Cp)_2ZrCl_2$ > Cp_2ZrCl_2 > $Me_2Si(Cp)_2ZrCl_2$ supported on H^+-mont-54.

Montmorillonite is readily available as a natural material and can be modified into a functional support for polymerization catalysts through appropriate chemical treatments. The resulting montmorillonite-based support can be applied to the development of MAO-free catalyst system. Recently, we explored an interesting application in which a hybrid catalyst system was developed by immobilizing zirconocene on the outer surface of montmorillonite and a bis(imino)pyridineiron complex within its interlayer space. This approach enabled the construction of a hybrid polymerization catalyst incorporating two different metal complexes [37].

CONFLICTS OF INTEREST

The authors declared that there is no conflict of interest.

REFERENCES

1. Pawlak M, Drzeżdżon J, Jacewicz D (2023) The greener side of polymers in the light of d-block metal complexes as precatalysts. Coord Chem Rev 484: 215122
2. Breil H, Holzkamp E, Martin H, Ziegler K (1960) Verfahren zur herstellung von hochmolekularen polyaethylenen. German Patent 973,626
3. Sinn H, Kaminsky W (1980) Ziegler-Natta catalysis. Adv Organomet Chem 18: 99-149
4. Sinn H, Kaminsky W, Vollmer H, Woldt R (1980) “Living polymers” on polymerization with extremely productive Ziegler catalysts. Angewandte Chem Int Ed Eng 19: 390-392
5. Kaminsky W (1996) New polymers by metallocene catalysis. Macromol Chem Phys 197: 3907-3945
6. Kaminsky W, Laban A (2001) Metallocene catalysis. Appl Catal A- Gen 222: 47-61
7. Yang X, Stern CL, Marks TJ (1994) Cationic zirconocene olefin polymerization catalysts based

on the organo-Lewis acid tris(pentafluorophenyl) borane. A synthetic, structural, solution dynamic, and polymerization catalytic study. J Am Chem Soc 116: 10015-10031
8. Ewen JA, Elder MJ (1991) Metallocene catalysts with Lewis acids and aluminum alkyls. EP Patent 0427697
9. Chen EYX, Marks TJ (2000) Cocatalysts for metal-catalyzed olefin polymerization: Activators, activation processes, and structure-activity relationships. Chem Rev 100: 1391-1434
10. Hlatky GG (2000) Heterogeneous single-site catalysts for olefin polymerization. Chem Rev 100: 1347-1376
11. Severn JR, Chadwick JC, Duchateau R, Friederichs N (2005) "Bound but Not gagged" immobilizing single-site α-olefin polymerization catalysts. Chem Rev 105: 4073-4147
12. Nifant'ev IE, Komarov PD, Kostomarova OD, Kolosov NA, Ivchenko PV (2023) MAO- and borate-free activating supports for group 4 metallocene and post-metallocene catalysts of α-olefin polymerization and oligomerization. Polymers 15: 3095
13. Kaminaka M, Soga K (1991) Polymerization of propene with the catalyst systems composed of Al_2O_3- or $MgCl_2$-supported $Et[IndH4]_2ZrCl_2$ and AlR_3 ($R = CH_3$, C_2H_5). Makromol Chem Rapid Commun 12: 367–372
14. Soga K, Kaminaka M (1993) Polymerization of propene with zirconocene-containing supported catalysts activated by common trialkylaluminiums. Makromol Chem 194: 1745-1755
15. Kissin YV, Nowlin TE, Mink RI, Brandolini AJ (2000) A new cocatalyst for metallocene complexes in olefin polymerization. Macromolecules 33: 4599-4601
16. Sun T, Garcés JM (2003) Acidic lamellar aerogel nanoplate activated olefin polymerization with metallocene catalysts. Catal Commun 4: 97-100
17. Chadwick JC, Severn JR (2006) Single-site catalyst immobilization using magnesium chloride supports. Kinet Catal 47: 186-191
18. Hicks JC, Mullis BA, Jones CW (2007) Sulfonic acid functionalized SBA-15 silica as a methylaluminoxane-free cocatalyst/support for ethylene polymerization. J Am Chem Soc 129: 8426-8427
19. Ikenaga K, Chen S, Ohshima M, Kurokawa H, Miura H (2007) Ethylene polymerization over zirconocenes supported on alumina- and titania-based acidic oxides. Catal Commun 8: 36-38
20. Huang R, Duchateau R, Koning CE, Chadwick JC (2008) Zirconocene immobilization and activation on $MgCl_2$-based supports: factors affecting ethylene polymerization activity. Macromolecules 41: 579-590
21. Yamamoto K (2009) Olefin polymerizations with zirconocene supported on SiO_2 modified by MgO, NaOH and LiOH. Appl Catal A- Gen 368: 65-70
22. Prades F, Broyer J, Belaid I, Boyron O, Miserque O, Spitz R, Boisson C (2013) Borate and MAO free activating supports for metallocene complexes. ACS Catal 3: 2288-2293
23. Tisse VF, Boisson C, McKenna TFL (2014) Activation and deactivation of the polymerization of ethylene over rac-$EtInd_2ZrCl_2$ and $(nBuCp)_2ZrCl_2$ on an activating silica support. Macromol Chem Phys 215: 1358-1369
24. Ochędzan-Siodłak W, Dziubek K (2014) Metallocenes and post-metallocenes immobilized on ionic liquid-modified silica as catalysts for polymerization of ethylene. Appl Catal A- Gen 484: 134-141
25. Panchenko VN, Danilova IG, Zakharov VA, Semikolenova NV, Paukshtis EA (2017) Effect of the acid–base properties of the support on the catalytic activity of ethylene polymerization using supported catalysts composed of Cp_2ZrX_2 (X = Cl, Me) and Al_2O_3(F). React Kinet Mech Catal 122: 275-287
26. Suga Y, Maruyama Y, Isobe E, Suzuki T, Shimizu F (1992) Katalysator für Olefinpolymerisation und Verfahren für Polyolefinproduktion. EP Patent 0511665
27. Suda Y, Suzuki T, Sugano T, Tayano T, Shimizu F (2002) Recent developments in transition metal-catalyzed polymerization I. Development of clay mineral-based metallocene catalyst. Kobunshi Ronbunshu 59: 178-189
28. Weiss K, Wirth-Pfeifer C, Hofmann M, Botzenhardt S, Lang H, Brüning K, Meichel E (2002) Polymerisation of ethylene or propylene with heterogeneous metallocene catalysts on clay minerals. J Mol Catal A- Chem 182-183: 143-149
29. Jeong DW, Hong DS, Cho HY, Woo SI (2003) The effect of water and acidity of the clay for ethylene polymerization over Cp_2ZrCl_2 supported on TMA-modified clay materials. J Mol Catal A-

Chem 206: 205-211
30. Tabernero V, Camejo C, Terreros P, Alba MD, Cuenca T (2010) Silicoaluminates as "support activator" systems in olefin polymerization processes. Materials 3: 1015-1030
31. Tayano T, Uchino H, Sagae T, Yokomizo K, Nakayama K, Ohta S, Nakano H, Murata M (2017) Effect of acid treatment of montmorillonite on "support-activator" performance to support metallocene for propylene polymerization catalyst. Macromol React Eng 11: 1600017
32. Kurokawa H, Morita S, Matsuda M, Suzuki H, Ohshima M, Miura H (2009) Polymerization of ethylene using zirconocenes supported on swellable cation-exchanged fluorotetrasilicic mica. Appl Catal A- Gen 360: 192-198
33. Tyumkina TV, Islamov DN, Parfenova LV, Whitby RJ, Khalilov LM, Dzhemilev UM (2016) Mechanistic aspects of chemo- and regioselectivity in Cp_2ZrCl_2-catalyzed alkene cycloalumination by $AlEt_3$. J Organomet Chem 822: 135-143
34. Tyumkina TV, Islamov DN, Parfenova LV, Karchevsky SG, Khalilov LM, Dzhemilev UM (2018) Mechanism of Cp_2ZrCl_2-catalyzed olefin cycloalumination with $AlEt_3$: Quantum chemical approach. Organometallics 37: 2406-2418
35. Nifant'ev IE, Vinogradov AA, Ivchenko PV (2021) Alternative mechanistic interpretation for unconventional catalytic behaviour of triisobutylaluminium-activated heterocenes in ethylene polymerization. Mendeleev Commun 31: 523-525
36. Tayano T, Uchino H, Sagae T, Ohta S, Kitade S, Satake H, Murata M (2016) Locating the active sites of metallocene catalysts supported on acid-treated montmorillonite. J Mol Catal A- Chem 420: 228-236
37. Kurokawa H, Otuki K, Fukuda T, Yamamoto K, Ogihara H (2025) Development of ternary hybrid ethylene polymerization catalysts composed of bis(imino)pyridineiron(III) complex, zirconocene, and Cr–montmorillonite. J Jpn Pet Inst 68: 177-186